Waste and Biomass Valorization (2024) 15:973–987
https://doi.org/10.1007/s12649-023-02210-8

ORIGINAL PAPER

Synthesis of Sulfonated Magnetic Nano-catalyst Using Rice Husk Ash for Corncob Hydrolysis: Kinetic and Thermodynamic Study

Olayomi Abiodun Falowo[1] · Oluwaseun O. Oyekola[2] · Babatunde Oladipo[2] · Abiola Ezekiel Taiwo[1] · Adeyosola Ilesanmi[1] · Oluwadabomi Davies[1]

Received: 26 November 2022 / Accepted: 14 June 2023 / Published online: 1 July 2023

Abstract

This study developed a magnetic solid acid catalyst for corncob hydrolysis. The core, Fe_3O_4 nanoparticle of the catalyst, was prepared using the co-precipitation method, which was supported by SiO_2 nanoparticles prepared from rice husk ash. The Fe_3O_4/C–SiO_2 was modified to produce a solid acid catalyst via the sulfonation method. Properties of Fe_3O_4/C and the sulfonated catalyst were assessed using FTIR, SEM, EDS, XRD, XPS, and VSM. Pretreated corncob was hydrolyzed at 80, 90, and 100 ^oC under a solid-to-liquid ratio of 1:10, using sulfonated Fe_3O_4/C for 100 min. Results showed that sulfonated Fe_3O_4/C–SiO_2 contained HSO_3 group indicating the success of the sulfonation process. The catalyst possessed a porous surface with a surface area of 72 m^2/g and a total acid density of 0.96 mmol/g. The hydrolysis rate of corncob increased with reaction time and temperature, with the highest total reducing sugar observed at 90 °C. Batch data obtained from the corncob hydrolysis using a solid catalyst can be described by Saeman's and integral first-order reaction models, establishing that cellulose hydrolysis is a first-order reaction. The activation energy for glucose formation was 12.33 and 42.4 kJ/mol for Saeman's and first-order reaction models, respectively. Thermodynamic parameters; ΔH, ΔS, and ΔG revealed that the hydrolysis process was thermodynamically favoured, and the glucose formation was more stable relative to the degradation products. Sulfonated Fe_3O_4/C–SiO_2 showed sustained activity after being reused four times.

✉ Olayomi Abiodun Falowo
falowo.olayomi@lmu.edu.ng

[1] Department of Chemical Engineering, Landmark University, P.M.B. 1001, Omu-Aran, Kwara State, Nigeria

[2] Department of Chemical Engineering, Cape Peninsula University of Technology, Bellville Campus, Symphony Way, Bellville, Cape Town 7535, South Africa

Graphical Abstract

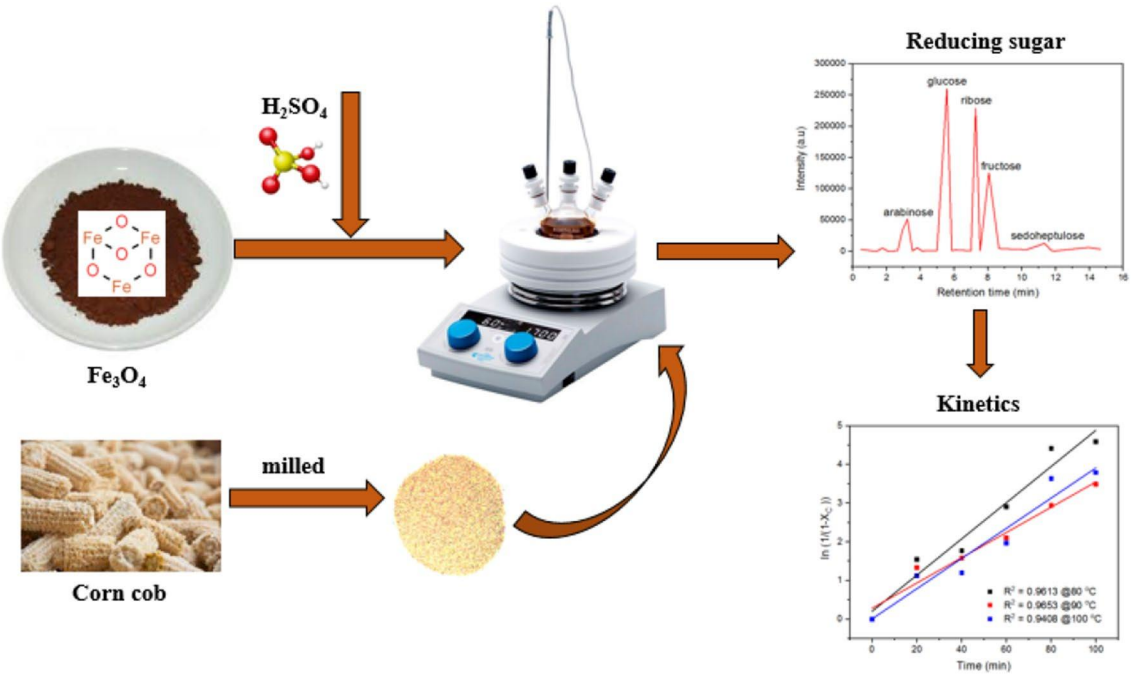

Keywords Corncob hydrolysis · Magnetic nanoparticle · Sulfonated nano-catalyst · Rice husk ash · Kinetics · Thermodynamics

Statement of Novelty

Effective biomass hydrolysis requires a detailed understanding of the mechanism of all involved components in the process. This study synthesized a magnetic solid acid catalyst to hydrolyze corncob residues in order to improve the separation process. In addition to catalyst development, the kinetics and thermodynamics of this process are vital for the optimal operation of hydrolysis reactors in biorefinery. The work focused on the utilization of acidified rice husk as a carbonaceous material to produce a solid acid catalyst through the sulfonation process. The recyclability of the acid catalyst was enhanced by using core magnetic nanoparticles. A lasting solid catalyst and high sugar recovery from corncob hydrolysis can be realized using this technology. The kinetic and thermodynamic parameters would enable the industrialists to design an efficient process for corncob hydrolysis.

Introduction

Production of alternative fuel and industrial raw materials from renewable sources continues to receive increased attention due to the growing concern over global warming. To that effect, an added value use of low-cost lignocellulosic resources has resulted in their application as economical raw materials in biofuel, pharmaceutical products, and cosmetics production [1, 2]. Generally, lignocellulosic biomass is a nonedible plant material generated at an enormous amount around the world which does not compete with food production. These include grass, corn stover, paper, wheat straw, wood residues, and agro-forest residues; having lignin, cellulose, and hemicellulose as the main components [3, 4]. Hydrolysis makes it possible to convert the lignocellulosic materials to fermentable sugars using acid catalysts or enzymes [3]. However, acid hydrolysis is advantageous over enzymatic hydrolysis because the rate of hydrolysis is faster, and acid can easily penetrate the lignin part without pretreatment [4]. Different acids have been applied in the literature to hydrolyze various lignocellulosic biomass. For example, dilute phosphoric acid was used in potato peel

hydrolysis [4], sulfuric acid in corn stover, switchgrass, and poplar wood hydrolysis [5], and formic acid in corncob hydrolysis [6].

In 2020, the Food and Agriculture Organization (FAO) statistics revealed that approximately 90.53 million tonnes of corn were produced in Africa [7], which accounted for 7.79% of the total corn production in the world. This makes corncobs to be one of the largest agricultural wastes in Africa. Corncob is an abundant and renewable bioresource generated after the processing of corn. The main composition of corncob residues is lignin (7–14%), cellulose (32.3–45%), and hemicellulose (38–39%) [8]. The products of corncob hydrolysis, such as levulinic acid, glucose, xylose, and furfural, have several applications, particularly in producing fuel and chemicals. For example, xylose, one of the main sugars in the hydrolysis solution of xylan-rich biomass, can be converted to xylitol. Xylitol is a functional sweetener having anti-cariogenic properties, reduced caloric value, protein stabilization effect, and negative thermal energy of dissolution [9]. In addition, xylose is the second-most abundant sugar on the earth and its bioconversion to bioethanol could provide an alternative source of energy [10].

The use of liquid mineral acids as catalysts for lignocellulose hydrolysis is unsustainable and impracticable since they are difficult to recover and recycle. Separating these catalysts is difficult and expensive, generating a huge amount of wastewater that must be further treated. Besides, corrosion of the reactor, sugar degradation, and safety concerns are common problems usually encountered [6]. Different types of solid acid catalysts have been investigated to solve the challenges of using liquid acids. They are categorized as carbon-based solid acids [11, 12], ZSM-5 Zeolite [13], inorganic salts [14], heteropoly acids [15], metal oxides and their complexes [16], acid cation exchange resins [17], and magnetic solid acid [18]. Considering the practical process of corncob hydrolysis using a solid catalyst, challenges remain that further complicate the process. Not all the solid catalysts developed can be readily recovered from the reaction mixture. In some processes, the amount of solid catalyst used for hydrolysis is higher than that of cellulose [18]. Also, hydrolysis must be conducted at a low cellulose/liquid ratio before a high yield of glucose can be obtained, which further increases the energy required to concentrate the product [18].

Given the inherent issues associated with using solid catalysts, magnetic carbon-based solid acid catalysts have been demonstrated to overcome these problems [19]. The catalyst after the hydrolysis reaction can be readily separated using an external magnet. Qi et al. [19] developed a magnetic carbon-based solid acid catalyst with high stability and catalytic performance. It was stated that the catalyst could be reused for up to 4 cycles in the pretreatment of the corncob. However, producing magnetic solid acid catalysts involves many expensive chemicals. The most commonly used method in the synthesis of this catalyst is via condensation of tetraethoxysilane (TEOS) and mercaptopropyltrimethoxysilane (MPTPMS). Not only that the chemicals are expensive, but they are not environmentally friendly, thereby constituting additional concern for the environment. For condensation, esterification, and hydrolysis; sulfonic group functionalized mesoporous silica materials are exceptional acid catalysts due to their hydrothermal stability [20]. Mesoporous silica nanoparticles are an excellent support for organic molecules due to properties such as high surface area and homogeneous pore channels [21]. Another biowaste rich in silica and/or silicon-containing compounds is rice husk biomass. Khazaei et al. [22] synthesized SiO_2 nanoparticles from rice husk. The synthesized SiO_2 was used to support palladium magnetic nanoparticles to produce a green catalyst for the Suzuki coupling reaction. A sulfurous magnetic solid acid catalyst having silica-based support has been applied in numerous synthesis reactions such as in the production of bis(pyrazolyl)methanes [23], indazolo[2, 1-b]phthalazine-triones [24], ester [25], reducing sugars [26], biodiesel [27], and glucose [28].

The hydrolysis rate of lignocellulosic biomass depends on reaction time, acid concentration, temperature, substrate amount and composition [4]. The kinetic parameters and the mechanism of cellulosic hydrolysis using dilute acid have been investigated severally in the past [29, 30]. The two proposed models are Saeman [31], for the hydrolysis of hemicellulosic fraction in wood and the two-fraction model [2]. The kinetics of hemicellulose hydrolysis in corncob using sulfuric acid has also been reported by Eken-Saracoglu et al. [32]. The study concluded that corncob hydrolysis follows a first-order reaction. In another study, the kinetic and thermodynamic parameters of corncob hydrolysis using dilute phosphoric acid were reported [8]. Liang et al. [33] studied simple kinetic models to describe corncob hydrolysis to levulinic acid using sulfuric acid. All these works on corncob hydrolysis and its kinetics were carried out using dilute mineral acids. The difficulties in recovering the catalyst from the solid mixture and the large amount of energy required for product concentration persist.

Hydrolysis of corncob has been carried out using different catalysts in literature, such as with carbonaceous solid acid catalyst synthesized from rice husk [34], as well as a magnetic carbon-based catalyst from microcrystalline cellulose [19] and bamboo [26]. Therefore, this study aimed to synthesize a magnetic biobased solid acid catalyst through sulfonation to expedite the hydrolysis of the corncob. The adopted approach of incorporating carbonaceous material of high silica content into the catalyst helped reduce the chemicals required during the catalyst synthesis. The catalyst preparation was modified through impregnation with nanoparticles developed from rice husk to ensure stability, and

the characteristics of the synthesized catalyst were detailed. The other objective of this present study was to establish the kinetics and thermodynamic parameters (an aspect that has been scarcely investigated in magnetic biobased solid acid hydrolysis of corncob). The findings would provide a better understanding of the chemical nature and further reveal additional insights into the corncob hydrolysis reaction mechanism.

Materials and Methods

Materials

The corncob and rice husk used for the experiment were collected from Landmark University Teaching Farm, Omu-Aran, Nigeria. The chemicals and reagents used in this study, such as Iron (III) chloride hexahydrate ($FeCl_3.6\ H_2O$), Iron (II) sulfate heptahydrate ($Fe_2SO_4.7\ H_2O$), ammonia solution (NH_4OH), ethanol, hydrochloric acid, acetone, phenolphthalein, sulfuric acid, and citric acid were all analytical grade. The chemicals were utilized without further purification.

Development of Rice husk Ash

SiO_2 nanoparticles were synthesized from rice husk through calcination. A rice husk of 50 g was washed in 1 M HCl and distilled water three times. The washed acid-leached rice husk was oven-dried at 100 °C for 2 h. The dried rice husk was loaded in a porcelain crucible and then calcined in a furnace at 650 °C for 3 h to obtain SiO_2 nanoparticles [22].

Synthesis of Core Fe_3O_4 Nanoparticles

The magnetic core (Fe_3O_4 nanoparticles) of the acid catalyst was prepared by co-precipitation according to Esfahani et al. [35]. In a typical batch synthesis, 200 mL of 0.2 M $FeCl_3{\cdot}6H_2O$ and 100 mL of 0.1 M $FeSO_4{\cdot}4H_2O$ were rapidly stirred in a round-bottomed flask placed on a hotplate operating at 80 °C. A 10 mL aqueous ammonia was added to the reacting mixture dropwise over 20 min to maintain the pH of the reaction at 12. The reaction mixture was rapidly stirred, and heated to a temperature of 85 °C which was maintained for 1 h. The black precipitates (iron oxide nanoparticles) were separated by magnetic decantation using a magnet after the mixture had cooled down. The resultant iron oxide was washed severally with distilled water, and then with ethanol, before it was dried at a moderate temperature in an oven for 4 h. The prepared iron nanoparticles were further encapsulated: 5 g of Fe_3O_4 were dissolved in 100 mL of 0.1 M citric acid solution. The reaction was maintained at 80 °C for 1 h while the resultant iron oxide-modified nanoparticles were precipitated with acetone. The citric acid-encapsulated iron oxide nanoparticles were magnetically separated and oven-dried at 80 °C.

Synthesis of Sulfonated Fe_3O_4/C Nano-catalyst

The biobased solid acid catalyst was prepared by following the steps described in Safari [36]. The SiO_2 nanoparticles prepared from the acidified rice husk and iron oxide nanoparticles were reacted in a mix of ethanol and de-ionized water (4:1) at a temperature of 50 °C for 6 h. Thereafter, the resulting Fe_3O_4/C–SiO_2 nanoparticles were magnetically decanted, dried, and stored for further analysis. The

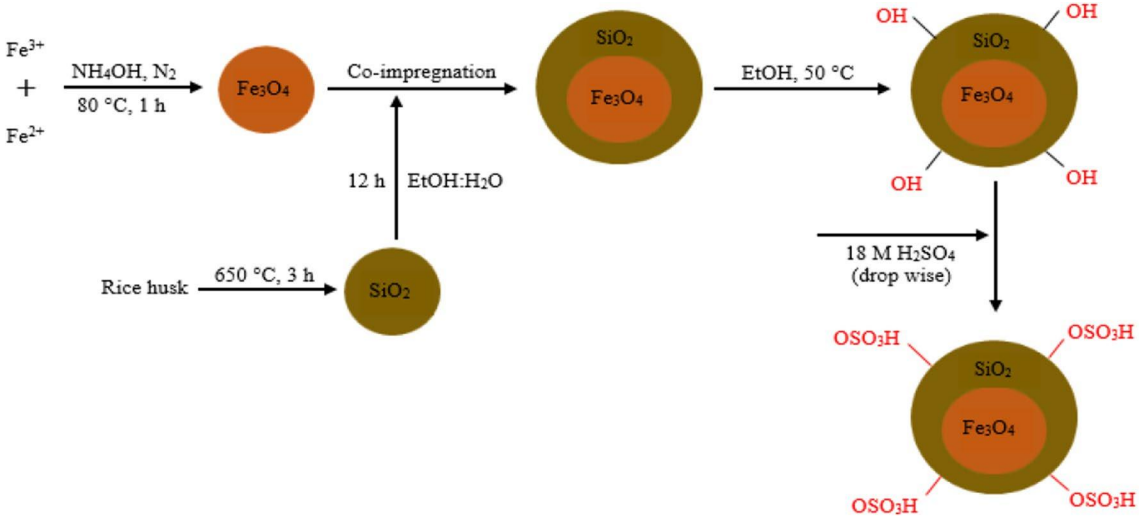

Fig. 1 Schematic diagram of the preparation of the magnetic solid acid catalyst

sulfonated Fe_3O_4/C was prepared by adopting the sulfonation method reported by Esfahani et al. [35]. In a typical batch process, 1 g of Fe_3O_4/C–SiO_2 was dispersed in 10 mL of hydrogen peroxide (30%) at room temperature. The mixture was stirred and concentrated sulfuric acid (18 M) was added in a drop-wise manner over 30 min. The resultant dispersion was moderately agitated for 4 h and the sulfonated Fe_3O_4/C–SiO_2 was separated and washed several times with methanol, then, finally dried in an oven at 80 °C for 4 h and stored for further use. The schematic illustration for the synthesis of a sulfurous-magnetic solid acid catalyst from Iron salts and rice husk is depicted in Fig. 1.

Characterization of Sulfonated Fe_3O_4/C–$SiO_2$and Fe_3O_4/C–SiO_2

Thermo Fisher Nova NanoSEM operating at 20 kV was used for Energy-dispersive X-ray spectroscopy (EDS) to determine the elemental composition of the synthesized samples. Surface morphology images of the samples were taken with a Tescan MIRA3 RISE. Fourier transform infrared (FTIR) spectra of sulfonated Fe_3O_4/C–SiO_2 and Fe_3O_4/C–SiO_2 were obtained with a PerkinElmer UATR Two spectrophotometer to determine the functional groups present. Chemical state and binding energy of the samples were obtained using X-ray photoelectron spectroscopy (XPS). The PHI 5000 scanning ESCA microprobe using monochromatic Al-Kα radiation was utilized to identify the binding energy peaks. Bruker D8-Advance diffractometer using Cu-Kα radiation was used for the X-ray diffraction (XRD) phase analysis of the samples. Cryogen Free Measurement System (CFMS) configuration was used for the measurement of the magnetic properties using a Vibrating Sample Magnetometer (VSM). Specific surface area of sulfonated Fe_3O_4/C was obtained using the Brunauer-Emmett-Teller (BET) method.

Surface Total Acid Density Determination

The total acid density on the surface of the sulfonated Fe_3O_4/C–SiO_2 catalyst was obtained by carrying out a neutralization titration [37]. The prepared sample (0.1 g) was dispersed into 1 M NaCl solution and the reaction mixture was sonicated for 30 min for sufficient ion exchange within the reacting species. Then, 50 mL of the supernatant was collected after the reaction, and a phenolphthalein indicator (3 drops) was added. The resulting solution was titrated against 0.1 M NaOH solution until the pH was neutral. The volume of NaOH solution consumed was recorded to determine the surface acid density (mmol/g) of sulfonated Fe_3O_4/C–SiO_2.

Proximate Analysis of Corncob

The proximate and compositional analyses of the screened corncob were established according to the National Renewable Energy Laboratory (NREL) procedures [38]. Using this method, moisture, volatile matter, ash, and fixed carbon contents of corncob were determined. The carbohydrate composition of corncob was determined according to the method outlined in Davis [39].

Hydrolysis of Milled Corncob

Corncob was washed, dried, and then milled in a milling machine. The milled corncob was screened by passing the particles through an 80 (177 µm) mesh screen. Hydrolysis experiment was carried out in a 500 mL three-necked batch reactor. The reactor was fitted with a reflux condenser and was positioned on a hotplate with a magnetic stirrer. The reaction was carried out under the following hydrolysis conditions; catalyst amount (1.0 g), reaction temperature (80, 90, and 100 °C), solid-liquid ratio (1:10), and reaction time (100 min). A known amount of milled corncob was weighed and transferred to the reactor, followed by the addition of distilled water according to the solid-to-liquid ratio, and thereafter, the mixture was homogenized for 5 min. The reaction mixture was heated to the desired temperature, followed by the addition of a defined quantity of solid acid catalyst, after which the reaction was allowed to run for the specified duration. After hydrolysis, the catalyst was subsequently separated from the reaction mixture with the aid of an external magnet. Residual solid was filtered with Whatman paper (pore size ˂ 2 µm), and the filtrate was analyzed to quantify the reducing sugar yield. The reducing sugar amount was determined by a 3,5-dinitro salicylic acid (DNS) method on a UV spectrophotometer. The absorbance of the filtrate was recorded at a wavelength of 540 nm.

The yield of reducing sugar was calculated using Eq. (1):

$$\%\ Total\ reducing\ sugar = \frac{moles\ of\ reducing\ sugar\ in\ the\ hydrolysate}{moles\ of\ reducing\ sugar\ in\ corncob} \times 100 \quad (1)$$

Reusability of Sulfonated Fe_3O_4/C Nano-catalyst

The reusability of sulfonated Fe_3O_4/C–SiO_2 was performed to test the stability of the synthesized catalyst. The hydrolysis experiment was conducted at 90 °C for 100 min. After each experiment, the catalyst was recovered by the external magnet, rinsed with distilled water, and subsequently applied in another hydrolysis step.

Reaction Kinetics, Activation Energy, and Thermodynamic Parameters of Corncob Hydrolysis

Kinetic study gives information about reaction mechanisms and it is crucial for the design and optimization of hydrolysis process parameters. The kinetic study of hydrolysis of cellulose in corncob was investigated by Saeman's model [31] and the integral method of data analysis by Levenspiel [40].

The generalized form of Saeman's model is shown in Eq. (2) [31].

$$Cellulose\ [C] \overset{k_1}{\rightarrow} Glucose\ [G] \overset{k_2}{\rightarrow} 5-HMF\ [H] \tag{2}$$

The analytical expressions of the resulting differential equation can be used to determine the concentrations of cellulose (C), glucose (G), and 5-hydroxymethylfurfural (H) as a function of time. This is shown in Eqs. (3)–(5)

$$C = C_0 e^{-k_1 t} \tag{3}$$

$$G = \frac{C_0 k_1}{k_2 - k_1}\left(e^{-k_1 t} - e^{-k_2 t}\right) \tag{4}$$

$$H = \left\{1 + \frac{k_1 e^{-k_2 t} - k_2 e^{-k_1 t}}{k_2 - k_1}\right\} C_0 \tag{5}$$

where, C_0 represents the amount of theoretical potential glucose available in corncob (g/L), rate constants k_1 (min^{-1}) and k_2 (min^{-1}) are zero under the initial concentration of products.

Assuming an irreversible reaction and negligible mass transfer rate effect across the catalyst surface, the experimental data were analyzed using unimolecular first-order reaction model as represented in Eq. (6).

$$\ln\left(\frac{1}{1 - X_C}\right) = kt \tag{6}$$

where, X_C, k, and t are the fractional conversion of cellulose to reducing sugar, the reaction rate constant, and the reaction time, respectively.

The activation energy is the minimum amount of energy required to initiate a chemical reaction. The activation energy of the hydrolysis reaction was determined from the natural logarithm of the Arrhenius equation as given in Eq. (7).

$$lnk = lnA - \frac{E_a}{RT} \tag{7}$$

where, k is the reaction rate constant (min^{-1}), A is the frequency factor (min^{-1}), E_a is the activation energy (kJ/mol), R is the universal gas constant (8.314 J/mol.K), and T is the absolute temperature (K).

Thermodynamic study helps in the prediction of parameters that govern the behaviour of chemical reactions and processes. The Erying-Polanyi equation to estimate the change in Gibbs free energy (ΔG)for the hydrolysis of corncob using sulfonated Fe_3O_4/C–SiO_2 catalyst is given in Eq. (8):

$$k = \kappa \frac{k_B T}{h} exp\left(-\frac{\Delta G}{RT}\right) \tag{8}$$

$$\Delta G = \Delta H - T\Delta S \tag{9}$$

Taking the natural logarithm of Eq. (8) and substituting Eq. (9) gives:

$$\ln\left(\frac{k}{T}\right) = -\frac{\Delta H}{R}\left(\frac{1}{T}\right) + \left[\ln\kappa + \ln\left(\frac{k_B}{h}\right) + \frac{\Delta S}{R}\right] \tag{10}$$

where, κ is the transmission coefficient with a value of one, k_B is the Boltzmann constant (1.38×10^{-23} J/K), and h is the Planck's constant (6.63×10^{-34} J.s). The values of enthalpy change (ΔH) and entropy change (ΔS) can respectively, be obtained from the slope and intercept of the linear plot of ln (k/T) vs. $1/T$.

Results and Discussion

Analyses of Sulfonated Fe_3O_4/C–SiO_2 and Fe_3O_4/C–SiO_2

The elemental composition of sulfonated Fe_3O_4/C–SiO_2 and Fe_3O_4/C–SiO_2 is presented in Table 1. The main elements are carbon, oxygen, silicon, and iron. The magnetic carboneceous sample (Fe_3O_4/C–SiO_2) without sulfonation showed no trace of sulfur (S1). As expected, the presence of C and Si in varrying amounts indicate that the synthesis methodology adopted was a success. The result illustrates that the S element is present in the sulfonated sample, indicating the

Table 1 Elemental composition of sulfonated Fe_3O_4/C–SiO_2 and Fe_3O_4/C–SiO_2

Sample	Composition (%)				
	C	O	Si	Fe	S
Sulfonated Fe_3O_4/C	22.36 ± 2.3	34.14 ± 3.4	6.32 ± 3.8	31.61 ± 5.4	5.56 ± 0.3
Fe_3O_4/C–SiO_2	24.63 ± 4.5	31.19 ± 5.4	7.47 ± 4.3	36.53 ± 4.9	–

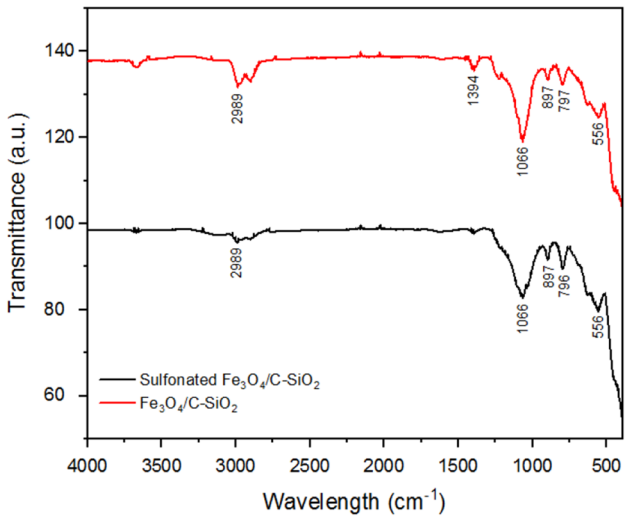

Fig. 2 FT-IR spectra of sulfonated Fe_3O_4/C–SiO_2 and Fe_3O_4/C–SiO_2

successful sulfonation of Fe_3O_4/C–SiO_2. During sulfonation, part of the S element formed a sulfone structure [41], hence, not all S element was present as –SO_3H group in the magnetic solid material.

The XRD pattern of the sulfonated Fe_3O_4/C–SiO_2 and Fe_3O_4/C–SiO_2 exhibited similar diffraction pattern which indicate that the core of materials is from the same source (S2). The diffraction pattern reveals the three dominant phases present in the sample which were indexed to reference patterns; goethite FeO(OH) (JCP: 81–0462), maghemite Fe_2O_3 (JCP: 39-1346), and magnetite Fe_3O_4 (JCP: 19–0629). The peak at 2θ = 21° illustrates the presence of an amorphous silica matrix in the sulfonated Fe_3O_4/C–SiO_2 and Fe_3O_4/C–SiO_2 samples [18]. The peaks at 2θ = 35, 53, and 63° have been identified in a similar magnetic solid acid catalysts. The weak diffraction peak at 2θ = 40–50° has been attributed to amorphous carbon formation [34]. No visible change and characteristic diffraction peaks are detected for

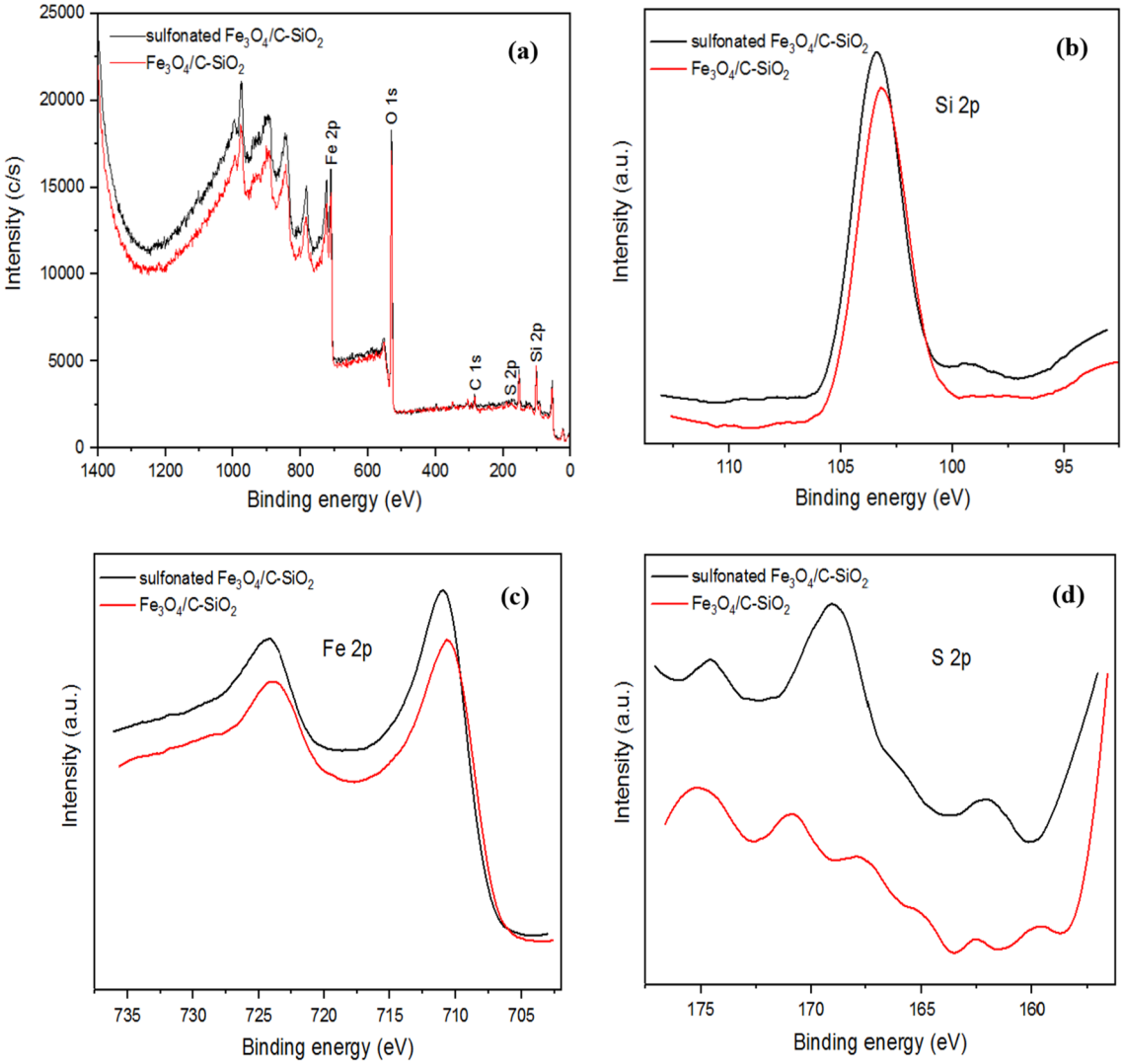

Fig. 3 XPS spectra of sulfonated Fe_3O_4/C–SiO_2 and Fe_3O_4/C–SiO_2

the sulfate group after sulfonation. A similar observation has also been reported in previous works [42, 43].

The FTIR spectra of sulfonated Fe_3O_4/C–SiO_2 and Fe_3O_4/C–SiO_2 samples in the region of 4000–400 cm^{-1} are shown in Fig. 2. An almost identical spectrum indicates the samples are made of similar compounds and the sulfonation did not affect the functional groups of Fe_3O_4/C–SiO_2. The vibration mode of the sulfate group is found between 980 and 1300 cm^{-1} [44]. However, this sometimes overlaps with Si–O–Si vibration occurring in the same region [45]. The band at 1066 and 897 cm^{-1} can be attributed to asymmetric stretching vibration and symmetric vibration of Si–O–Si, respectively. The band at 2989 cm^{-1} was assigned to aliphatic CH stretching vibration [21]. Broad band extending from 1066 to 1200 cm^{-1}, though not prominent corresponds to the asymmetric stretching of S=O [45].

The XPS analysis of Fe_3O_4/C–SiO_2 and sulfonated Fe_3O_4/C–SiO_2 were further studied to validate the surface species of the solid acid catalyst. The wide survey scan of the XPS spectra is presented in Fig. 3a. The presence of iron, sulfur, and oxygen are well indicated. According to the high-resolution XPS spectra, a little chemical shift occurred after sulfonation. In the spectra of C 1s (S3), the peaks at binding energies of 285.2 eV (sulfonated Fe_3O_4/C–SiO_2) and 284.9 eV (Fe_3O_4/C) are indicative of the C = O carbon, showing the carbonates of the samples. The Si 2p spectra (Fig. 3b) showed peaks at binding energies of 103.4 eV (sulfonated Fe_3O_4/C) and 103.2 eV (Fe_3O_4/C–SiO_2), which indicate that Si was present in the form of silicates or silica in the sample. The observed peaks at binding energies of 532.4 eV (sulfonated Fe_3O_4/C–SiO_2) and 532.1 eV (Fe_3O_4/C–SiO_2) in the spectra of O 1s (S4) are both indicative of the elemental oxygen of the hydroxides and sulfate groups present in the samples. The O 1s doublet consists of two peaks differing by ~3 eV in the binding energy. These peaks are wide and asymmetric which indicates the presence of O atom in two oxidation states. In another acid catalyst, similar peaks are ascribed to O^{2-} and oxygen in H_2O molecules [46]. In the Fe 2p spectra (Fig. 3c), two doublets (i.e., Fe $2p_{1/2}$ and Fe $2p_{3/2}$) were observed. The most intense peak (Fe $2p_{3/2}$) of the Fe 2p doublet revealed peaks at 710.9 eV (sulfonated Fe_3O_4/C–SiO_2) and 710.6 eV (Fe_3O_4/C–SiO_2), which were attributed to the binding energy of Fe(III)–O chemical state. The peaks further indicate that the Fe atom was present as Fe^{2+} and Fe^{3+} in the excited state. In the spectra of S 2p (Fig. 3d), there is a notable change in the peak intensity after sulfonation. Sulfonated Fe_3O_4/C–SiO_2 sample showed an intense signal at 169.0 eV, which can be attributed to the presence of sulfate ions (SO_4^{2-}). This binding energy value agrees with the report presented in Hino et al. [47] and can be assumed to explain the chemical shift observed in O 1s after sulfonation. This revealed the S^{6+} of SO_4^{2-} in the synthesized catalyst which is responsible for the acidity on the surface of sulfonated Fe_2O_4/C–SiO_2. Thus, the presence of the sulfate group further showed a successful sulfonation.

Using VSM, the magnetic properties of the samples were established. The hysteresis loop of sulfonated Fe_3O_4/C–SiO_2 and Fe_3O_4/C–SiO_2 at different temperatures are depicted in Fig. 4. The two types of hysteresis loops were similar, with saturation magnetization intensity of 0.14 and 0.20 emu/g for sulfonated Fe_3O_4/C–SiO_2 and Fe_3O_4/C–SiO_2, respectively. It can be observed that the magnetism intensity was

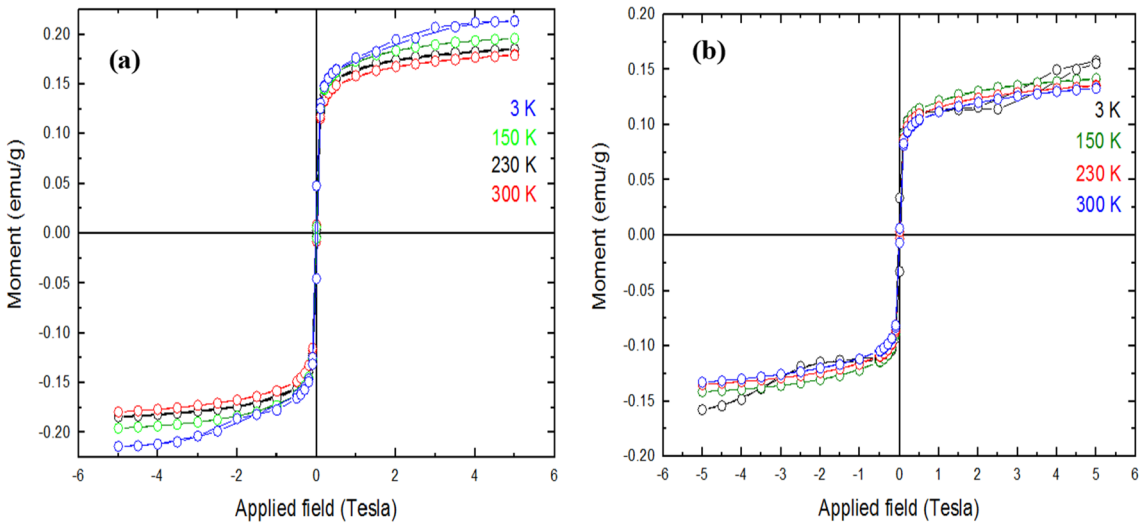

Fig. 4 VSM analysis of **a** sulfonated Fe_3O_4/C–SiO_2 and **b** Fe_3O_4/C–SiO_2

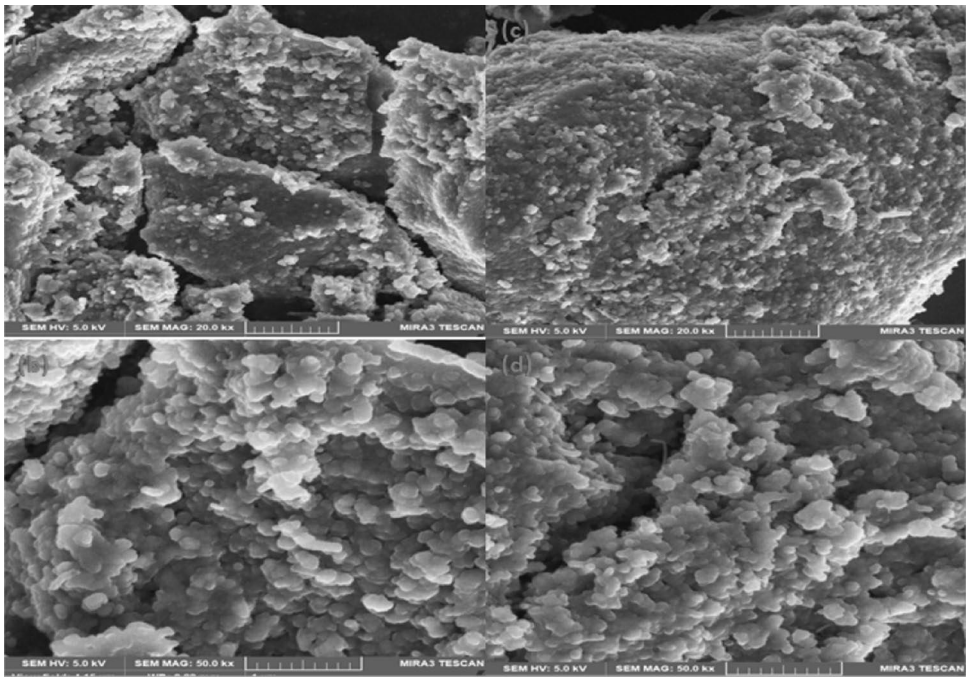

Fig. 5 SEM images of sulfonated Fe_3O_4/C–SiO_2 at **a** 20 kx, **b** 50 kx, and Fe_3O_4/C–SiO_2 nanoparticles at **c** 20 kx and **d** 50 kx

not affected by further modification with acid. Though, the super-paramagnetism activity of Fe_3O_4/C–SiO_2 reduces after sulfonation with sulfuric acid. However, this might make it hard for Fe_3O_4/C–SiO_2 to reassemble during the reaction, thus leading to a better dispersion [48] as the hydrolysis progresses.

The surface morphology of the sulfonated Fe_3O_4/C–SiO_2 and Fe_3O_4/C–SiO_2 samples at 20 and 50 kx magnifications are presented in Fig. 5. It can be observed that the regular particle shapes are present in both samples, an indication that the synthesized nanoparticles might have high porosity which is vital for heterogeneous catalysis. The SEM images of sulfonated catalyst possessed uniform spherical agglomerates. At a magnification of 20 kx, the sulfonated Fe_3O_4/C–SiO_2 surface was fractured, which indicates that the pore size of the active site still maintained its dimension even after sulfonation. Similar surface morphologies have been reported for the catalyst modified by the sulfate group [45].

The specific surface area of sulfonated Fe_3O_4/C–SiO_2 as determined by BET was 72 m^2/g. The value obtained in our study is higher than the reported value of 68.5 m^2/g obtained from sulfonated magnetic carbon nanoparticles [49]. This result indicates that the catalyst surface has sufficient dimension to allow passage of reacting species which could enhance the diffusion of reactant in and out of the catalyst active site making it suitable for a heterogeneous catalysis system. The estimated surface acid density of the sulfonated catalyst was 0.96 mmol/g, which is greater than the value reported by Qi et al. [19] in their work on magnetic carbon-based solid acid treatment for corncob saccharification.

Proximate Analysis and Chemical Composition of Corncob

The proximate analysis and the lignocellulosic composition of raw corncob residue are volatile matter of 75 wt%, cellulose of 47.36 wt%, hemicellulose of 38.38 wt%, and lignin of 10.5 wt%. The values obtained for volatile matter and fixed carbon (S5) are in the range of the values reported for lignocellulosic materials in Wijaya et al. [50]. The total amount of cellulose and hemicellulose was ~ 86% of the lignocellulosic component. This further highlights the usefulness of corncob in biorefinery processes as a source of fermentable sugars. The hemicellulose, cellulose, and lignin were in the range reported by other studies [51, 52].

Results of Hydrolysis of Corncob

The reaction mechanism of the corncob hydrolysis using synthesized catalyst is shown in Fig. 6. The strong covalent and weak hydrogen bonding networks of both cellulose and hemicellulose chains were cleaved by the SO_3^{2-} group of the catalyst to release reducing sugars. The total reducing sugar recover from the hydrolysis process using the sulfonated Fe_3O_4/C–SiO_2 is found in S6. The reducing sugar recovery increased with hydrolysis time in all the temperatures investigated. Figure 7 depicts the net reducing sugars obtained from the hydrolysis of the corncob. The net reducing sugar increases with time and it shows that none of the reactions

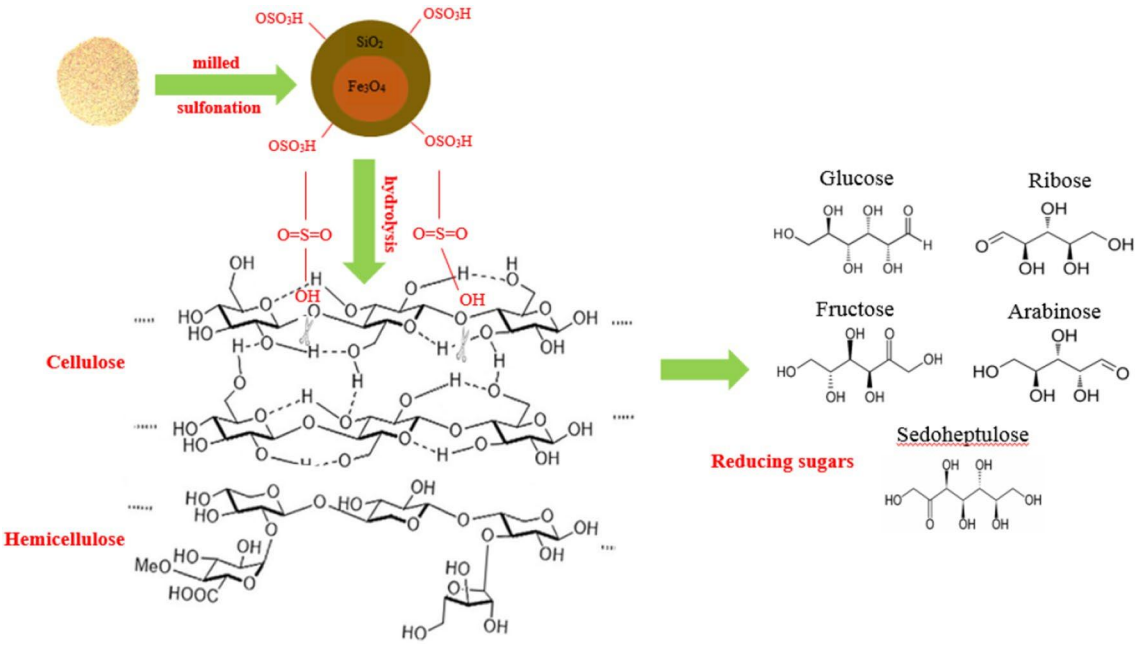

Fig. 6 Mechanism of action for corncob hydrolysis using Magnetic solid acid catalyst

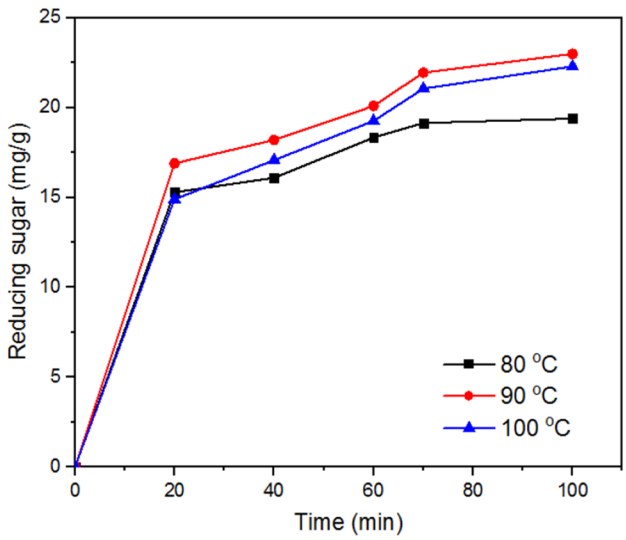

Fig. 7 Plot of total reducing sugar against time

goes to completion. The total sugar produced increased with an increase in temperature; for a 10 °C increase from the initial temperature, the total reducing sugar recovered was high. However, a further increase in temperature from 90 to 100 °C led to a reduction in the total amount of sugar recovered. The decrease in total sugar amount at 100 °C might be due to the evaporation of water from the reaction mixture. This behaviour is consistent with the report of Gómora-Hernández et al. [8].

The chromatogram of the hydrolysate at 90 °C revealed the presence of both hexose and pentose sugars (S7). The reducing sugars in the sample are mainly glucose and ribose, while a weak intensity of sedoheptulose is detected. Gómora-Hernández et al. [8] reported that different sugars can be produced from corncob hydrolysis depending on the hydrolysis condition. The study categorized this condition as most severe (1.34 M H_3PO_4, 110 °C, and 5 h) and less severe (0.58 M H_3PO_4, 90 °C, and 0.5 h).

Table 2 Magnetic solid acid catalyst applied in hydrolysis

Catalyst	Biomass	Carbon-based material	Acid	Total acidity (mmol/g)	Yield of reducing sugar (%)	References
Fe_3O_4/C–SO_3H	corncob	anhydrous glucose	sulfuric acid	1.66	44.3 (xylose)	Zhang et al. [53]
MMCSA	corncob	microcrystalline cellulose	sulfuric acid	0.85	90.4	Qi et al. [19]
SMCNs	fructose	eucalyptus oil	sulfuric acid	–	51.6 (5-HMF)	Le et al. [49]
Fe_3O_4-SBA-SO_3H	corncob	SBA-15	TEOS, MTPMS		45	Lai et al. [18]
Sulfonated Fe_3O_4/C– SiO_2	corncob	Rice husk	sulfuric acid	0.96	82.3	This study

MMCSA magnetic carbon-based solid acid, *SMCNs* sulfonated magnetic carbon nanoparticles

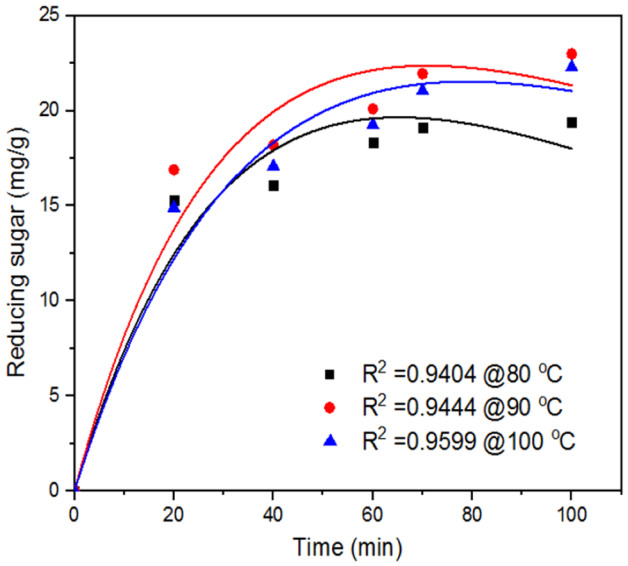

Fig. 8 Reducing sugar as a function of time (Saeman's model)

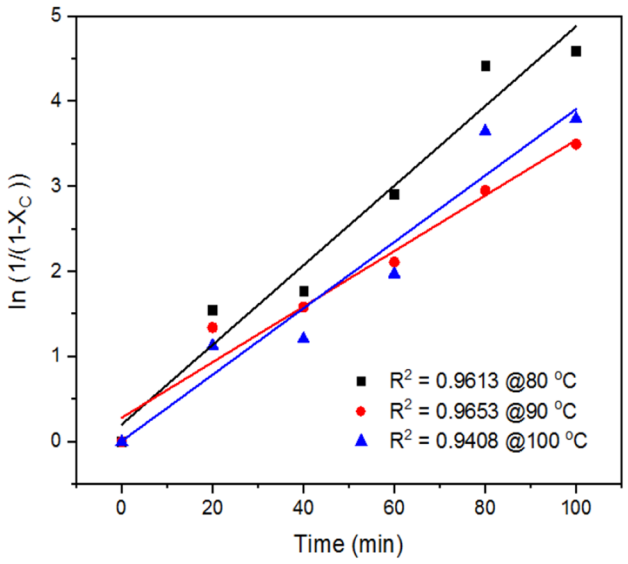

Fig. 9 First-order rate reaction of corncob hydrolysis

In the first 20 min of the corncob hydrolysis, over 50% of the reducing sugar was recovered at all temperatures. Since hydrolysis of hemicellulose in corncob occurs easily over a short period compared to the cellulose portion [31], the high sugar amount at this reaction time could be assumed to come from hemicellulose. Extension of hydrolysis time from 20 to 40 min shows a marginal increase in sugar recovery and a further increase in time resulted in rapid sugar recovery. This observation is consistent with cellulose hydrolysis in a closed system. The performance of the catalyst synthesized in this study was compared with other solid acid catalysts used for corncob hydrolysis (Table 2).

Table 3 Rate constants from Saeman's (k_1, k_2) and first-order (k) reaction models

Rate constants	80 °C	90 °C	100 °C
k_1 (min^{-1})	0.0271	0.0306	0.03226
k_2 (min^{-1})	0.00483	0.0059	0.00746
k_1/k_2	5.611	5.186	4.324
k (min^{-1})	0.02072	0.03267	0.03903

Table 4 Kinetic and thermodynamics parameters of corncob hydrolysis

Parameters	Rate constants		
	k_1 (glucose formation)	k_2 (glucose degradation)	k (first-order reaction model)
Kinetic			
A (min^{-1})	1.77	186	3524
E_a (kJ/mol)	12.33	31.50	42.40
Thermodynamics			
ΔH(kJ/mol)	8.68	27.89	40.94
ΔS(J/mol.K^{-1})	− 527.59	− 479.82	− 438.95
ΔG(kJ/mol)	199.97	202.06	200.27

A–frequency factor, E_a–activation energy, ΔH–change in enthalpy, ΔS–change in entropy, ΔG–change in Gibb's free energy

Kinetic Analysis Of Corncob Hydrolysate

The batch hydrolysis data obtained were fitted using the model equations presented in Eqs. (3–6). Saeman's model was used to fit the total reducing sugar as a function of time (Fig. 8). At high reaction time, the net reducing sugar was not linear as was observed at lower reaction time. There is a clear deviation that suggests that the rate of degradation of reducing sugar to 5-HMF is faster than the initial reaction time. When the temperatures were 80 and 90 °C, the reducing sugar showed a marginal decline at a high reaction time. This trend is consistent with the observation reported by Adeogun et al. [30]. Unlike total reducing sugar at lower temperatures, at 100 °C the total sugar seems to be constant as the reaction progresses.

The integral first-order reaction model was used to describe the experimental data obtained (Fig. 9). The hydrolysis data fitted well at all temperatures as revealed by the high R^2 values. The data fitness at 90 °C suggests that this temperature could be the optimum value for corncob hydrolysis using sulfonated Fe_3O_4/C–SiO_2. Although, the value of R^2 obtained using these two models is high (~ 1), however, both models gave optimum values at different

temperatures. The R^2 of Saeman's model was highest at 100 °C ($R^2 = 0.9599$) while the R^2 was highest at 90 °C ($R^2 = 0.9653$) for the first-order rate model. Generally, hydrolysis of lignocellulosic materials is a complex process due to the rate of different degradation products [8, 33], which is not taken into consideration in the first-order reaction model. In both models, the R^2 of the reaction at 100 °C is almost the same with a slight difference of 0.019. This could mean that at lower temperatures, total reducing sugar might be overestimated.

The rate constants determined from corncob hydrolysis using sulfonated Fe_3O_4/C–SiO_2 are presented in Table 3. It can be observed that k_1 increases relative to k_2 at all temperatures. For a 10 °C increase in temperature, k_1 increases approximately twice the value of k_2. It was reported that glucan depolymerization to glucose was faster than glucose decomposition from the value of rate constants [54].

A direct comparison of rate constant values in this study with the values obtained in other studies is difficult due to the temperature differences investigated and the kinetic models used. In the production of levulinic acid from corncob, the rate constants of 0.00367 min^{-1} and 0.00581 min^{-1} were obtained for glucose formation and decomposition to 5-HMF, respectively [33]. The logarithms of the rate constants are plotted against the reciprocal of the absolute temperature (S8). The linearity observed indicates that the reaction follows Arrhenius expression, relating the hydrolysis rate to the reaction temperature. The frequency factor and activation energy were evaluated from the linear equations generated from these plots.

The kinetic parameters at different rate constant values are presented in Table 4. The activation energies in this study were relatively low compared to the 96 kJ/mol activation energy reported by Wang et al. [54] when Lewis acid ($FeCl_3$) was used. Adeogun et al. [30] reported activation energy of 6.12 and 10.16 kJ/mol for glucose formation and glucose degradation, respectively, for pretreated corncob hydrolysis using $ZnCl_2$ enhanced acid catalyst.

The thermodynamic parameters of cellulose hydrolysis and glucose degradation determined from both models are presented in Table 4. The logarithm plots of the ratio of rate constants to absolute temperature against the reciprocal of absolute temperature were used to evaluate the thermodynamic parameters (S9). The positive value of ΔH is an indication that glucose formation from corncob hydrolysis is an endothermic process. The obtained value of 27.89 kJ/mol indicates that higher energy thrice of the value required for glucose formation is required for degradation. This observation is similar to the trend reported by Adeogun et al. [30]. The ΔH obtained using a first-order model indicates that more energy is required for hydrolysis. The negative value of ΔS was estimated for glucose formation and degradation product. The more negative the value of ΔS, the higher the stability of the product formed. It can be observed that the product of hydrolysis is more stable relative to the degradation product. The value of ΔG obtained for glucose degradation was higher than the value estimated for corncob hydrolysis. This indicates that glucose formation is thermodynamically favoured over glucose degradation. This trend is in uniformity with the observation reported by Gurgel et al. [55]. It was also observed that the ΔG values of glucose formation using Saeman's model and the first-order reaction model are approximately the same.

Reusability of Sulfonated Fe_3O_4/C–SiO_2

The reusability potential of the synthesized catalyst was high, as depicted in its plot (S10). This test was carried out at 90 °C and a solid:liquid ratio 1:10 for 100 min. The sulfonated Fe_3O_4/C–SiO_2 can be reused for four hydrolysis cycles with a negligible loss of its activity. At the end of the 4th cycle, the total reducing sugar decreased by 21% due to the ineffectiveness of the catalyst. The decline in the activity of the synthesized nano-catalyst could be attributed to the partial leaching of the –SO_3H functional group and the blockage of catalyst active sites by humins generated in the hydrolysis process [34, 56]. Li et al. [57] reported the reuse of magnetic RuCo nanoparticles up to four cycles in ammonia borane hydrolysis, and Lai et al. [18] recycled magnetic solid acid catalyst three times from corncob hydrolysis with no significant loss of performance.

Conclusion

A magnetic solid acid nano-catalyst was successfully synthesized through co-precipitation and sulfonation methods. The core magnetic nanoparticle was prepared from Fe salts, and the synthesis of Fe_3O_4 nanoparticles was further modified by impregnating them with calcined rice husk ash, followed by sulfonation with concentrated sulfuric acid. The sulfonated Fe_3O_4/C–SiO_2 was successfully applied to hydrolyze corncob at 80, 90, and 100 °C. The synthesized catalyst possessed excellent catalytic activity having a surface area of 72 m^2/g and a mesoporous surface with an acid density of 0.96 mmol/g. The total reducing sugar recovery from the corncob was highest at 90 °C. The hydrolysis data fitted using Saeman's model and integral first-order reaction model established that both models are consistent in describing corncob hydrolysis rate. This further aids the understanding of the mechanism involved in corncob hydrolysis. The activation energy for glucose formation is 12.33 and 42.4 kJ/mol for Saeman's and first-order reaction models, respectively. The thermodynamics parameters; ΔH, ΔS, and ΔG revealed that the hydrolysis process was thermodynamically favoured, and

the glucose formation was more stable relative to degradation products. The sulfonated Fe_3O_4/C–SiO_2 catalyst was reused four times in corncob hydrolysis. Thus, the catalyst (sulfonated Fe_3O_4/C–SiO_2) could solve the problems encountered in lignocellulose hydrolysis since its synthesis is inexpensive and environmentally friendly.

Supplementary Information The online version contains supplementary material available at https://doi.org/10.1007/s12649-023-02210-8.

Acknowledgements The authors appreciate the inputs of the Soil Science Laboratory Staff and the Chemical Engineering Technologists, Landmark University, Omu-Aran, Nigeria.

Author Contributions OF: conceptualization, supervision, original draft preparation, visualization. OO: reviewing and editing, resources. BO: data curation, original draft preparation, reviewing, and editing. AT: supervision. AI: investigation, methodology. OD: investigation, methodology. All authors read and approved the final manuscript.

Funding This research did not receive any financial support from funding organizations in the public, commercial, or not-for-profit sectors.

Data Availability The data supporting the current study are available within the article.

Declarations

Competing interests The authors have no relevant financial or non-financial interests to disclose.

Ethical Approval The results presented in this manuscript are the original works of the authors. This manuscript has not been published in a journal outlet in any form or language. The authors all contributed to the completion of this work. The findings presented were conveyed without any falsification or misrepresentation of data. All references used in this study were properly acknowledged, and all rules guiding a good scientific practice were maintained to ensure professionalism.

References

1. Zakzeski, J., Grisel, R.J., Smit, A.T., Weckhuysen, B.M.: Solid acid-catalyzed cellulose hydrolysis monitored by situ ATR-IR spectroscopy. ChemSusChem **5**(2), 430–437 (2012)
2. Gámez, S., Ramírez, J.A., Garrote, G., Vázquez, M.: Manufacture of fermentable sugar solutions from sugar cane bagasse hydrolyzed with phosphoric acid at atmospheric pressure. J. Agric. Food Chem. **52**(13), 4172–4177 (2004)
3. Verardi, A., De Bari, I., Ricca, E., Calabrò, V.: Hydrolysis of lignocellulosic biomass: current status of processes and technologies and future perspectives. In: Bioethanol, pp. 95–122. InTech, Rijeka (2012)
4. Lenihan, P., Orozco, A., O'Neill, E., Ahmad, M., Rooney, D., Walker, G.: Dilute acid hydrolysis of lignocellulosic biomass. Chem. Eng. J. **156**(2), 395–403 (2010)
5. Gao, X., Kumar, R., Wyman, C.E.: Fast hemicellulose quantification via a simple one-step acid hydrolysis. Biotechnol. Bioeng. **111**(6), 1088–1096 (2014)
6. Zhu, T., Li, P., Wang, X., Yang, W., Chang, H., Ma, S.: Optimization of formic acid hydrolysis of corn cob in xylose production. Korean J. Chem. Eng. **31**(9), 1624–1631 (2014)
7. FAOSTAT. Food and Agriculture Organization of the United Nations.: Statistics Division 2020. www.fao.org/faostat/en/#data/QC (2020). Accessed on 10 2022
8. Gómora-Hernández, J.C., Carreño-de-León, M.C., Flores-Alamo, N., Hernández-Berriel, M.C., Fernández-Valverde, S.M.: Kinetic and thermodynamic study of corncob hydrolysis in phosphoric acid with a low yield of bacterial inhibitors. Biomass Bioenerg. **143**, 105830 (2020)
9. Parajó, J.C., Domínguez, H., Domínguez, J.: Biotechnological production of xylitol. Part 1: interest of xylitol and fundamentals of its biosynthesis. Bioresour. Technol. **65**(3), 191–201 (1998)
10. Jeffries, T.W.: Engineering yeasts for xylose metabolism. Curr. Opin. Biotechnol. **17**(3), 320–326 (2006)
11. Li, X., Shu, F., He, C., Liu, S., Leksawasdi, N., Wang, Q., Qi, W., Alam, M.A., Yuan, Z., Gao, Y.: Preparation and investigation of highly selective solid acid catalysts with sodium lignosulfonate for hydrolysis of hemicellulose in corncob. RSC Adv. **8**(20), 10922–10929 (2018)
12. Qi, W., He, C., Wang, Q., Liu, S., Yu, Q., Wang, W., Leksawasdi, N., Wang, C., Yuan, Z.: Carbon-based solid acid pretreatment in corncob saccharification: specific xylose production and efficient enzymatic hydrolysis. ACS Sustain. Chem. Eng. **6**(3), 3640–3648 (2018)
13. Hoang, P.H., Chung, N.H., Dien, L.Q.: Porous ZSM-5 zeolite catalyst modified with sulfonic acid functional groups for hydrolysis of biomass. J. Iran. Chem. Soc. **16**(10), 2203–2210 (2019)
14. Mao, L., Zhang, L., Gao, N., Li, A.: FeCl3 and acetic acid co-catalyzed hydrolysis of corncob for improving furfural production and lignin removal from residue. Bioresour. Technol. **123**, 324–331 (2012)
15. Gromov, N.V., Medvedeva, T.B., Rodikova, Y.A., Pestunov, A.V., Zhizhina, E.G., Taran, O.P.: The production of formic acid from polysaccharides and biomass via one-pot hydrolysis-oxidation in the presence of Mo-VP heteropoly acid catalyst. J. Siberian Fed. Univ. Chem. **11**(1), 56–71 (2018)
16. Cheng, L., Liu, H., Cui, Y., Xue, N., Ding, W.: Direct conversion of corn cob to formic and acetic acids over nano oxide catalysts. J. energy Chem. **23**(1), 43–49 (2014)
17. Lehrfeld, J.: Conversion of agricultural residues into cation exchange materials. J. Appl. Polym. Sci. **61**(12), 2099–2105 (1996)
18. Lai, D., Deng, L., Li, J., Liao, B., Guo, Q., Fu, Y.: Hydrolysis of cellulose into glucose by magnetic solid acid. ChemSusChem. **4**(1), 55–58 (2011)
19. Qi, W., Liu, G., He, C., Liu, S., Lu, S., Yue, J., Wang, Q., Wang, Z., Yuan, Z., Hu, J.: An efficient magnetic carbon-based solid acid treatment for corncob saccharification with high selectivity for xylose and enhanced enzymatic digestibility. Green Chem. **21**(6), 1292–1304 (2019)
20. Van Rhijn, W., De Vos, D., Sels, B., Bossaert, W.: Sulfonic acid functionalised ordered mesoporous materials as catalysts for condensation and esterification reactions. Chem. Commun. **3**, 317–318 (1998)
21. Khalifa, M.E., Abdelrahman, E.A., Hassanien, M.M., Ibrahim, W.A.: Application of mesoporous silica nanoparticles modified with dibenzoylmethane as a novel composite for efficient removal of cd (II), hg (II), and Cu (II) ions from aqueous media. J. Inorg. Organomet. Polym. Mater. **30**(6), 2182–2196 (2020)
22. Khazaei, A., Khazaei, M., Nasrollahzadeh, M.: Nano-Fe3O4@SiO2 supported pd (0) as a magnetically recoverable nanocatalyst for Suzuki coupling reaction in the presence of waste eggshell as low-cost natural base. Tetrahedron. **73**(38), 5624–5633 (2017)
23. Mohammadi, M., Ghorbani-Choghamarani, A.: Hercynite silica sulfuric acid: a novel inorganic sulfurous solid acid catalyst for one-pot cascade organic transformations. RSC Adv. **12**(40), 26023–26041 (2022)

24. Kiasat, A.R., Davarpanah, J.: Fe3O4@ silica sulfuric acid nanoparticles: an efficient reusable nanomagnetic catalyst as potent solid acid for one-pot solvent-free synthesis of indazolo [2, 1-b] phthalazine-triones and pyrazolo [1, 2-b] phthalazine-diones. J. Mol. Catal. A: Chem0 **373**, 46–54 (2013)
25. Jenie, S.A., Kristiani, A., Kustomo, Simanungkalit, S., Mansur, D.: Preparation of nanobiochar as magnetic solid acid catalyst by pyrolysis-carbonization from oil palm empty fruit bunches. In: AIP Conference Proceedings. AIP Publishing LLC, Melville (2017)
26. Zhu, Y., Huang, J., Sun, S., Wu, A., Li, H.: Effect of dilute acid and alkali pretreatments on the catalytic performance of bamboo-derived carbonaceous magnetic solid acid. Catalysts. **9**(3), 245 (2019)
27. Wang, Y.-T., Yang, X.-X., Xu, J., Wang, H.-L., Wang, Z.-B., Zhang, L., Wang, S.-L., Liang, J.-L.: Biodiesel production from esterification of oleic acid by a sulfonated magnetic solid acid catalyst. Renew. Energy **139**, 688–695 (2019)
28. Hu, S.-L., Zeng, Y.-J., Wu, D.-Z., Lou, W.-Y.: A novel magnetic carbon-based solid acid catalyst suitable for efficient hydrolysis of cellulose. Biomass Conv. Bioref. (2021). https://doi.org/10.1007/s13399-020-01240-9
29. Xiang, Q., Lee, Y.Y., Torget, R.W.: Kinetics of glucose decomposition during dilute-acid hydrolysis of lignocellulosic biomass. In: Proceedings of the Twenty-Fifth Symposium on Biotechnology for Fuels and Chemicals Held May 4–7, 2003, in Breckenridge, CO. Humana Press, Totowa (2004)
30. Adeogun, A., Agboola, B., Idowu, M., Shittu, T.: ZnCl2 enhanced acid hydrolysis of pretreated corncob for glucose production: kinetics, thermodynamics and optimization analysis. J. Bioresour. Bioprod. **4**(3), 149–158 (2019)
31. Saeman, J.F.: Kinetics of wood saccharification-hydrolysis of cellulose and decomposition of sugars in dilute acid at high temperature. Industrial Eng. Chem. **37**(1), 43–52 (1945)
32. Eken-Saraçoğlu, N., Mutlu, S.F., Dilmaç, G., Çavuşoğlu, H.: A comparative kinetic study of acidic hemicellulose hydrolysis in corn cob and sunflower seed hull. Bioresour. Technol. **65**(1–2), 29–33 (1998)
33. Liang, C., Hu, Y., Guo, L., Wu, L., Zhang, W.: Kinetic study of acid hydrolysis of corncobs to levulinic acid. BioResources. **12**(2), 4049–4061 (2017)
34. Chen, N., Zhang, G., Zhang, P., Tao, X., Wu, Y., Wang, S., Nabi, M.: Rice husk-based solid acid for efficient hydrolysis and saccharification of corncob. Bioresour. Technol. **292**, 121915 (2019)
35. Esfahani, F.K., Zareyee, D., Yousefi, R.: Sulfonated core-shell magnetic nanoparticle (Fe3O4@ SiO2@ PrSO3H) as a highly active and durable protonic acid catalyst; synthesis of coumarin derivatives through Pechmann reaction. ChemCatChem. **6**(12), 3333–3337 (2014)
36. Safari, J., Zarnegar, Z.: A highly efficient magnetic solid acid catalyst for synthesis of 2, 4, 5-trisubstituted imidazoles under ultrasound irradiation. Ultrason. Sonochem. **20**(2), 740–746 (2013)
37. Quah, R.V., Tan, Y.H., Mubarak, N., Kansedo, J., Khalid, M., Abdullah, E., Abdullah, M.O.: Magnetic biochar derived from waste palm kernel shell for biodiesel production via sulfonation. Waste Manage. **118**, 626–636 (2020)
38. Sluiter, A., Hames, B., Ruiz, R., Scarlata, C., Sluiter, J., Templeton, D., Crocker, D.: Determination of structural carbohydrates and lignin in biomass. Lab. Anal. proced. **1617**(1), 1–16 (2008)
39. Davis, M.W.: A rapid modified method for compositional carbohydrate analysis of lignocellulosics by high pH anion-exchange chromatography with pulsed amperometric detection (HPAEC/PAD). J. Wood Chem. Technol. **18**(2), 235–252 (1998)
40. Levenspiel, O.: Chemical Reaction Engineering. Wiley, Hoboken (1998)
41. Hara, M.: Biodiesel production by amorphous carbon bearing SO3H, COOH and phenolic OH groups, a solid Brønsted acid catalyst. Top. Catal. **53**(11), 805–810 (2010)
42. Kitano, M., Arai, K., Kodama, A., Kousaka, T., Nakajima, K., Hayashi, S., Hara, M.: Preparation of a sulfonated porous carbon catalyst with high specific surface area. Catal. Lett. **131**(1), 242–249 (2009)
43. Nda-Umar, U.I., Ramli, I., Muhamad, E.N., Taufiq-Yap, Y.H., Azri, N.: Synthesis and characterization of sulfonated carbon catalysts derived from biomass waste and its evaluation in glycerol acetylation. Biomass Convers. Biorefinery **12**, 1–16 (2020)
44. Navarrete, J., Lopez, T., Gomez, R., Figueras, F.: Surface acidity of sulfated TiO2–SiO2 sol-gels. Langmuir **12**(18), 4385–4390 (1996)
45. Shao, G.N., Sheikh, R., Hilonga, A., Lee, J.E., Park, Y.-H., Kim, H.T.: Biodiesel production by sulfated mesoporous titania–silica catalysts synthesized by the sol–gel process from less expensive precursors. Chem. Eng. J. **215**, 600–607 (2013)
46. Dziembaj, R., Małecka, A., Piwowarska, Z., Bielański, A.: XPS study of polyaniline supported dodecatungstosilicic acid catalyst. J. Mol. Catal. A: Chem. **112**(3), 423–430 (1996)
47. Hino, M., Kurashige, M., Matsuhashi, H., Arata, K.: The surface structure of sulfated zirconia: studies of XPS and thermal analysis. Thermochim. Acta **441**(1), 35–41 (2006)
48. Wang, T., Lin, J., Chen, Z., Megharaj, M., Naidu, R.: Green synthesized iron nanoparticles by green tea and eucalyptus leaves extracts used for removal of nitrate in aqueous solution. J. Clean. Prod. **83**, 413–419 (2014)
49. Le, G.T., Arunaditya, K., Panichpol, J., Rodruangnon, T., Thongratkaew, S., Chaipojjana, K., Faungnawakij, K., Charinpanitkul, T.: Sulfonated magnetic carbon nanoparticles from eucalyptus oil as a green and sustainable catalyst for converting fructose to 5-HMF. Catal. Commun. **149**, 106229 (2021)
50. Wijaya, Y.P., Putra, R.D.D., Widyaya, V.T., Ha, J.-M., Suh, D.J., Kim, C.S.: Comparative study on two-step concentrated acid hydrolysis for the extraction of sugars from lignocellulosic biomass. Bioresour. Technol. **164**, 221–231 (2014)
51. Zhang, H.-J., Fan, X.-G., Qiu, X.-L., Zhang, Q.-X., Wang, W.-Y., Li, S.-X., Deng, L.-H., Koffas, M.A., Wei, D.-S., Yuan, Q.-P.: A novel cleaning process for industrial production of xylose in pilot scale from corncob by using screw-steam-explosive extruder. Bioprocess Biosyst. Eng. **37**(12), 2425–2436 (2014)
52. Xue, J.W., Wang, Z.A.: Study on catalytic hydrolysis of corncob by formic acid. In: advanced materials research. Trans Tech Publ. **560**, 321–324 (2012)
53. Zhang, X., Tan, X., Xu, Y., Wang, W., Ma, L., Qi, W.: Preparation of core-shell structure magnetic carbon-based solid acid and its catalytic performance on hemicellulose in corncobs. BioResources. **11**(4), 10014–10029 (2016)
54. Wang, C., Yang, G., Zhang, X., Shao, L., Lyu, G., Mao, J., Liu, S., Xu, F.: A kinetic study on the hydrolysis of corncob residues to levulinic acid in the FeCl3–NaCl system. Cellulose. **26**(15), 8313–8323 (2019)
55. Gurgel, L.V.A., Marabezi, K., Zanbom, M.D., Curvelo, A.A.S.: Dilute acid hydrolysis of sugar cane bagasse at high temperatures: a kinetic study of cellulose saccharification and glucose decomposition. Part I: sulfuric acid as the catalyst. Ind. Eng. Chem. Res. **51**(3), 1173–1185 (2012)
56. Jiang, Y., Li, X., Wang, X., Meng, L., Wang, H., Peng, G., Wang, X., Mu, X.: Effective saccharification of lignocellulosic biomass over hydrolysis residue derived solid acid under microwave irradiation. Green Chem. **14**(8), 2162–2167 (2012)
57. Li, X., Zeng, C., Fan, G.: Magnetic RuCo nanoparticles supported on two-dimensional titanium carbide as highly active catalysts for the hydrolysis of ammonia borane. Int. J. Hydrog. Energy. **40**(30), 9217–9224 (2015)